

Nature of the global fluctuations in the spherical model at criticality

Jean-Yves Fortin and Sophie Mantelli

CNRS, Institut Jean Lamour, Département de Physique de la Matière et des Matériaux, UMR 7198, Vandoeuvre-les-Nancy, F-54506, France

E-mail: fortin@ijl.nancy-universite.fr, smantell@ijl.nancy-universite.fr

Abstract. We study the universal nature of global fluctuations in the critical regime of the spherical model by evaluating the exact distribution of the magnetization and its absolute value in the thermodynamical limit, in the presence of a conjugate field. We show that the probability distribution function for this model is described by non-Gaussian asymptotics and non-symmetric characteristics which depend on the dimension of the system $2 < d < 4$. Relation with extreme statistics of independent wavelength modes is discussed.

PACS numbers: 05.70.Jk, 05.40.-a, 05.50.+q, 68.35.Rh

1. Introduction

Global fluctuations of space-averaged order parameters in many statistical systems possess generally a non-gaussian behavior in their critical and non-mean field regime. One well-known example is given by the two-dimensional XY-model (2D-XY), whose magnetic fluctuations (specifically the absolute value of the global spin vector) can be studied within the spin-wave approximation on the low-temperature critical line [1, 2, 3], far enough from the Kosterlitz-Thouless transition [4, 5, 6]. One interesting feature and universal character of the resulting rescaled probability distribution function (PDF) is that it does not depend on the critical exponents, temperature and system size [7]. Moreover the exponential and double exponential asymptotic fall-off behaviors for negative and positive deviations respectively, up to some corrective terms, identify this PDF to a general Gumbel function parametrized by a non-integer. Gumbel functions describe the extrema distribution of a set of independent and identically distributed Gaussian variables. They are parametrized by an integer which is equal to one for the lowest value, two for the second lowest values and so on. The connection with the 2D-XY-model is based on the existence of low excitations modes, the Goldstone modes, which tend to destroy the quasi-long range order at low temperature. In Fourier space, the modes of value \mathbf{q} , are decoupled and have a mass linearly proportional to $|\mathbf{q}|$, and therefore the low soft modes are the predominant contributions to the PDF, giving rise to a strongly non-Gaussian behavior and Gumbel limiting distribution with non-integer parameter $\pi/2$. Simple one dimensional and self-critical models such as interface distribution or $1/f$ noise [8] give also a Gumbel distribution with parameter equal to one and therefore strongly non-Gaussian. Gumbel distributions with generalized parameter are also common in one-dimensional non-equilibrium and correlated systems where the distribution can be cast into a product of single probabilities with independent but non-identically distributed variables [9, 10]. In all these example, the Fourier modes have mass proportional to $|\mathbf{q}|$, therefore leading to the same limiting distribution dominated by the soft modes. This function is constructed by isolating the non-singular part of the fluctuations when the system size is taken to infinity, usually this is done by rescaling the order parameter using the mean value and variance only. Self-organized systems [11, 12] and network applications are also important systems in the way that they often lead to exact mathematical results [13, 14], for example the distribution of connectivity in random graphs [15], width distribution of interfaces [16], or size distributions in replicative phenomena [17, 18]. Generally, one expects to approach the critical point from the low temperature region where the distribution for the order parameter m (for example the magnetization per site in a spin system) can be generally written as $P(m, L) = L^{\beta/\nu} Q(mL^{\beta/\nu}, \xi/L, hL^{\beta\delta/\nu})$, where ξ is the correlation length, h an external field conjugated to the order parameter m , L the typical system size and Q the limiting or asymptotic PDF independent of L . The critical exponents (β, δ, ν) depend on the specific model. For the classical 2D-XY model, where m is defined as the modulus of the total spin vector divided by the number of sites L^2 , this asymptotic distribution can

be very closely written as [3]

$$Q(\theta) \simeq \exp\left(-\frac{1}{8\pi}e^{8\pi\left(\sqrt{g_2/2\theta-a_0}\right)} + 8\pi\sqrt{\frac{g_2}{2}\theta}\right) \quad (1)$$

with $a_0 = 1/24 + \gamma/(4\pi) - \ln(4\pi)/(4\pi) - \ln \prod_{k=1}^{\infty} [1 - \exp(-2\pi k)]/(2\pi) \simeq 0.113514$, and constant $g_2 \simeq 3.867 \times 10^{-3}$. Here $\theta = (m- < m >)/\sigma$, with σ^2 the variance, is the standard rescaled parameter for defining correctly the non-singular limit. The asymptotic regimes when $|\theta|$ is large are important in defining the class of function where the PDF belongs to. For independent and identically distributed fluctuations, the PDF falls into the Gaussian class. Otherwise, the PDF usually falls into class of functions characteristic of generalized extreme value statistics, for example Gumbel, Weibull or Fréchet [19]. They are however few correlated systems where the asymptotic PDF of global order parameter can be evaluated analytically [20, 3] and where the effect of the correlations can be measured. In this paper we focus essentially on the critical regime of a simple correlated spin-model, the well-known spherical model in dimension $2 < d < 4$ [21], where fluctuations of the order parameter (magnetization and its absolute value) can be studied exactly in the critical regime. This will give some physical insight on universal features belonging to critical correlated systems.

2. Definition of the Model

We consider the spherical model [21] defined by a set of $N = L^d$ scalar spins $-\infty < S_i < +\infty$ coupled together with nearest-neighbor ferromagnetic coupling J_{ij} on a d -dimensional lattice at temperature $T = 1/\beta$. The spins are constraint by the condition $\sum_i S_i^2 = N$, and the Hamiltonian is given by

$$H_0 = -\frac{1}{2} \sum_{i,j} J_{ij} S_i S_j, \quad (2)$$

with $J_{ij} = J \sum_{\alpha} \delta_{\mathbf{r}_i, \mathbf{r}_j \pm \mathbf{e}_{\alpha}}$ where $\mathbf{e}_{\alpha=1, \dots, d}$ are the unit spacing vectors of the lattice. For example, in $d = 2$, $\mathbf{e}_1 = \mathbf{x}$ and $\mathbf{e}_2 = \mathbf{y}$. Following the standard techniques, see [21, 22], the partition function is written using a Dirac delta function representation to impose the constraint on the spins

$$Z_N(h) = \int \frac{ds}{2\pi} \int_{-\infty}^{+\infty} \prod_{\mathbf{r}_i} dS_i \exp \left[-\beta H_0 + h \sum_i S_i + (is + a) \left(N - \sum_i S_i^2 \right) \right] \quad (3)$$

where a is any arbitrary real scalar which does not change the value of the integral over s . The successive derivatives of $Z_N(h)$ with respect to h give the moments of the magnetization $m := \sum_i S_i/N$ which we want to study. We will also consider another partition function by replacing the field term $h \sum_i S_i$ by $\bar{h} |\sum_i S_i|$, and from which we

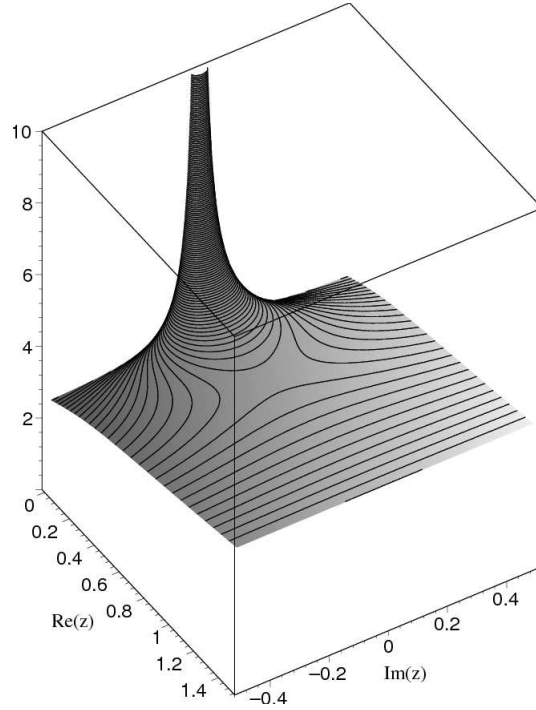


Figure 1. Surface plot of the function $\Phi(z, h)$ (vertical axis) in the complex plane, showing the location of the unique saddle point. Here $h = K = 1$ and $N = 10^3$ in $d = 3$.

can derive the successive moments of the absolute value of the magnetization $|m|$. In general we can consider both fields and study the different moments from $Z_N(h, \bar{h})$. The integration over the S_i can be done using Fourier transform $S_i = \frac{1}{\sqrt{N}} \sum_{\mathbf{q}} S_{\mathbf{q}} e^{i\mathbf{q} \cdot \mathbf{r}_i}$, with $S_{-\mathbf{q}} = \bar{S}_{\mathbf{q}}$, $\mathbf{q} = 2\pi(k_1, \dots, k_d)/L$, and $k_i = 0, \dots, L-1$. In this case the interaction term can be diagonalized directly such as

$$\frac{\beta}{2} \sum_{i,j} J_{ij} S_i S_j = K \sum_{\mathbf{q}} S_{\mathbf{q}} S_{-\mathbf{q}} \sum_{\alpha} \cos q_{\alpha}$$

with $K := \beta J$. After Fourier transformation, the constraint contribution becomes simply

$$(is + a) \sum_i S_i^2 = \frac{(is + a)}{N} \sum_i \sum_{\mathbf{q}, \mathbf{q}'} S_{\mathbf{q}} S_{\mathbf{q}'} e^{i(\mathbf{q} + \mathbf{q}') \cdot \mathbf{r}_i} = (is + a) \sum_{\mathbf{q}} S_{\mathbf{q}} S_{-\mathbf{q}}. \quad (4)$$

The other linear terms are equal to $h \sum_i S_i = h\sqrt{N} S_0$, and $\bar{h} |\sum_i S_i| = \bar{h}\sqrt{N} |S_0|$. We can finally express the partition function as an integral over a product of decoupled Fourier modes

$$Z_N(h, \bar{h}) = \int \frac{ds}{2\pi} \int_{-\infty}^{+\infty} dS_0 \prod'_{\mathbf{q} \neq 0} dS_{\mathbf{q}} dS_{-\mathbf{q}} \exp \left[-K \sum_{\mathbf{q}} S_{\mathbf{q}} S_{-\mathbf{q}} \left(z + d - \sum_{\alpha} \cos q_{\alpha} \right) \right]$$

$$+ h\sqrt{N}S_0 + \bar{h}\sqrt{N}|S_0| + NK(z+d)] \quad (5)$$

where $K(z+d) = is + a$. a is chosen to avoid the integral divergence for the zero mode. The prime symbol on the product means that only half of the Fourier modes are considered, using the symmetry $\mathbf{q} \rightarrow -\mathbf{q}$. Decomposing $S_{\mathbf{q}} = x_{\mathbf{q}} + iy_{\mathbf{q}}$ in real and imaginary parts, so that $dS_{\mathbf{q}}dS_{-\mathbf{q}} = dx_{\mathbf{q}}dy_{\mathbf{q}}$, $S_{\mathbf{q}}S_{-\mathbf{q}} = x_{\mathbf{q}}^2 + y_{\mathbf{q}}^2$, we obtain after integration over Fourier modes the integral expression of the partition function

$$Z_N(h, \bar{h}) = \int \frac{ds}{2\pi} \left(\frac{\pi}{2K} \right)^{N/2} \exp \left[-\frac{1}{2} \sum_{\mathbf{q}} \ln \left(z + d - \sum_{\alpha} \cos q_{\alpha} \right) + N \frac{h^2 + \bar{h}^2}{4Kz} + NK(z+d) \right] \\ \times \frac{1}{\sqrt{2}} \left[2 \cosh \frac{h\bar{h}}{2Kz} + e^{-Nh\bar{h}/(2Kz)} \operatorname{erf} \left(\frac{\sqrt{N}(\bar{h} - h)}{2\sqrt{Kz}} \right) + e^{Nh\bar{h}/(2Kz)} \operatorname{erf} \left(\frac{\sqrt{N}(\bar{h} + h)}{2\sqrt{Kz}} \right) \right].$$

From this expression, we can define the intensive free energy $\Phi(z, h, \bar{h})$ for the system such that

$$Z_N(h, \bar{h}) = \int \frac{ds}{2\pi} \left(\frac{\pi}{2K} \right)^{N/2} \sqrt{2} \exp [N\Phi(z, h, \bar{h})] \quad (6)$$

with, for each of the two order parameters considered in this paper

$$\Phi(z, h, 0) = -\frac{1}{2N} \sum_{\mathbf{q}} \ln \left(z + d - \sum_{\alpha} \cos q_{\alpha} \right) + \frac{h^2}{4Kz} + K(z+d), \quad (7) \\ \Phi(z, 0, \bar{h}) = -\frac{1}{2N} \sum_{\mathbf{q}} \ln \left(z + d - \sum_{\alpha} \cos q_{\alpha} \right) + \frac{\bar{h}^2}{4Kz} + K(z+d) + \frac{1}{N} \ln \left[1 + \operatorname{erf} \left(\frac{\sqrt{N}\bar{h}}{2\sqrt{Kz}} \right) \right].$$

It is clear that Φ is not an even function of \bar{h} for the absolute value of magnetization. As N is large, we can study the saddle points of Φ in the complex plane, and obtain the main contributions to the free energy and partition function.

3. Saddle point analysis and scaling relations in the critical region

In Figure 1, we represented Φ for some arbitrary values of parameters, which shows the location of the unique saddle point as the minimum of Φ along the real z -axis, which is also a maximum along the real s -axis or imaginary z -axis. In particular the equation of the local saddle point satisfies for example

$$\frac{\partial \Phi(z, h, 0)}{\partial z} = -\frac{1}{2N} \sum_{\mathbf{q} \neq 0} \frac{1}{z + d - \sum_{\alpha} \cos q_{\alpha}} - \frac{1}{2Nz} - \frac{h^2}{4Kz^2} + K = 0. \quad (8)$$

The last equation gives the implicit saddle point solution $z(h)$ as function of field h . The critical point $K = K_c$ is defined by $K_c := \lim_{N \rightarrow \infty} \frac{1}{2N} \sum_{\mathbf{q} \neq 0} (d - \sum_{\alpha} \cos q_{\alpha})^{-1} =:$

$\frac{1}{2}g_1$, after taking first the limit $N \rightarrow \infty$ then $h = 0$ and finally $z = 0$. This quantity is well defined for $d > 2$. In two dimensions for example, this quantity is pertinent for characterizing the XY model and diverges with the system size as $g_1 \simeq (1/2\pi) \log(CN)$ [3] with the exact value

$$C = \exp \left\{ \frac{\pi}{3} + 2 \log \left(\frac{\sqrt{2}}{\pi} \right) + 2\gamma - 4 \log \prod_{n=1}^{\infty} [1 - \exp(-2\pi n)] \right\} \simeq 1.8456$$

The evaluation of this constant requires a precise analysis of the discrete sum over the Fourier modes which is specific to the geometry of the lattice. By extension it is useful to define the dimension-dependent quantities

$$g_p := \frac{1}{N^p} \sum_{\mathbf{q} \neq 0} \frac{1}{(d - \sum_{\alpha} \cos q_{\alpha})^p} =: \frac{1}{N^p} \sum_{\mathbf{q} \neq 0} G_{\mathbf{q}}^p \quad (9)$$

which scale with L in the large size limit, and where $G_{\mathbf{q}}$ is the Green function. Indeed, in the interval $2 < d < 4$, we can replace the sum over modes \mathbf{q} by an integral and show that

$$g_p \approx \frac{1}{N^p} \int_{\text{cst}/L}^{q_{\max}} \frac{L^d}{(2\pi)^d} G_{\mathbf{q}}^p q^{d-1} dq, \quad (10)$$

where q_{\max} is some cut-off dependent of the lattice step. The integrand is dominant when q is small, precisely $G_{\mathbf{q}} \propto q^{-2}$, then $g_p \approx L^{d(1-p)} [q^{d-2p}]_{\text{cst}/L}^{q_{\max}}$. If $p = 1$, the integral is convergent for $d > 2$, and g_1 is finite, as well as the critical temperature. Otherwise, for $p \geq 2$, $d - 2p$ is strictly negative if $d < 4$, and the integration part $[q^{d-2p}]_{\text{cst}/L}^{q_{\max}}$ is dominated by L^{2p-d} which is divergent. Therefore g_p scales like $L^{d(1-p)+2p-d} = L^{-p(d-2)}$ and goes to zero like

$$g_{p \geq 2} = \tilde{g}_p L^{-p(d-2)} + O(L^{-d(p-1)}), \quad \tilde{g}_p := \lim_{L \rightarrow \infty} \frac{1}{L^{2p}} \sum_{\mathbf{q} \neq 0} G_{\mathbf{q}}^p, \quad (11)$$

where \tilde{g}_p are finite and positive constants. The corrective terms $O(L^{-d(p-1)})$ are always negligible since $2p > d$, which holds when $2 < d < 4$. The case $d = 2$ is particular since all g_p are finite, except for g_1 which diverges logarithmically with L as it was discussed above. These constants are actually essential for evaluating the PDF of the 2D-XY model [3] as they are related to the moments of the distribution. For example, magnetization goes slowly to zero with the system size like $\langle m \rangle = (NC)^{-T/(8\pi)} = e^{-Tg_1/2}$. The important point is that these constants depend only on dimension and lattice geometry.

The scaling exponents of the spherical model in the range $2 < d < 4$ are given by $\alpha = -(4-d)/(d-2)$, $\beta = 1/2$, $\gamma = 2/(d-2)$, $\delta = (d+2)/(d-2)$, and $\nu = 1/(d-2)$.

They satisfy the scaling relations $\alpha + 2\beta + \gamma = 2$, $\alpha = 2 - d\nu$, and $\gamma = \nu(2 - \eta)$. In the critical region, we define therefore the rescaled parameters

$$K - K_c =: k_0 L^{-1/\nu} = k_0 L^{-(d-2)}, \quad h =: h_0 L^{-\beta\delta/\nu} = h_0 L^{-(d+2)/2}, \quad (12)$$

where k_0 (which can be negative, in the paramagnetic region) and h_0 are external parameters. Similarly, \bar{h} follows the same scaling as h , or $\bar{h} =: \bar{h}_0 L^{-(d+2)/2}$. Therefore the magnetization scales like $\langle m \rangle \propto (K - K_c)^\beta \propto h^{1/\delta} \propto L^{-(d-2)/2}$. These arguments imply that the different moments and cumulants of order p scale like $\langle m^p \rangle \propto L^{-p(d-2)/2}$ in the critical region. Cumulants κ_p can be computed using the successive derivatives of Φ :

$$\kappa_p = \frac{1}{N^{p-1}} \frac{d^p \Phi}{d h^p} =: \tilde{\kappa}_p L^{-p(d-2)/2}, \quad (13)$$

and the asymptotic distribution defined in the introduction can be identified with the function Q using a Fourier transform (see Appendix A)

$$Q(\theta) := \int \frac{d\lambda}{2\pi} \exp \left[i\lambda\theta + \sum_{p \geq 2} \frac{\tilde{\kappa}_p}{\tilde{\kappa}_2^{p/2}} \frac{(-i\lambda)^p}{p!} \right], \quad (14)$$

which is independent of the system size. We first evaluate the saddle point solution of Equation (8), using the scaling Equation (12) and assuming z small:

$$\begin{aligned} & -\frac{1}{2N} \sum_{\mathbf{q} \neq 0} \frac{1}{d - \sum_{\alpha} \cos q_{\alpha}} + \frac{z}{2N} \sum_{\mathbf{q} \neq 0} \frac{1}{(d - \sum_{\alpha} \cos q_{\alpha})^2} + \dots - \frac{1}{2Nz} \\ & - \frac{h_0^2}{4K_c z^2} L^{-(d+2)} + K_c + k_0 L^{-(d-2)} + \dots = 0. \end{aligned} \quad (15)$$

A first analysis of the previous equation leads to the identification of the scaling law $z \sim L^{-2}$ since for example $z^{-2} L^{-(d+2)} \sim L^{-(d-2)}$ by comparison of terms on the second line. All other terms scale with the same exponent $2 - d$. This means that $\partial\Phi/\partial z$ scales like $L^{-(d-2)}$ and $\Phi \sim L^{-d}$ at the critical point. Therefore the solution $z(h)$ can be expanded as a series in the inverse power of L : $z(h) = L^{-2} z_0 + \dots$ (and $z(\bar{h}) = L^{-2} \bar{z}_0 + \dots$ as well). We obtain at the leading order $O(L^{-(d-2)})$

$$\begin{aligned} & -\frac{1}{2} g_1 + \frac{1}{2} z_0 \tilde{g}_2 L^{-(d-2)} - \frac{1}{2} z_0^2 \tilde{g}_3 L^{-(d-2)} + \frac{1}{2} z_0^3 \tilde{g}_4 L^{-(d-2)} - \dots \\ & - \frac{1}{2z_0} L^{-(d-2)} - \frac{h_0^2}{4K_c z_0^2} L^{-(d-2)} + K_c + k_0 L^{-(d-2)} = 0. \end{aligned} \quad (16)$$

The zeroth order term $K_c = g_1/2$ is canceled, and we obtain an implicit equation for $z_0 = z_0(k_0, h_0)$ and $\bar{z}_0 = \bar{z}_0(k_0, \bar{h}_0)$ as function of the reduced temperature and magnetic field:

$$-\frac{1}{2z_0} + \frac{1}{2}z_0\tilde{g}_2 - \frac{1}{2}z_0^2\tilde{g}_3 + \frac{1}{2}z_0^3\tilde{g}_4 - \dots = \frac{h_0^2}{4K_c z_0^2} - k_0, \quad (17)$$

and a similar expansion for \bar{z}_0 as well. We can express the previous equation in a more compact form, using the definition of the \tilde{g}_p s and summing the series over p

$$-\frac{1}{2z_0} + \frac{1}{2} \sum_{\mathbf{q} \neq 0} \frac{z_0 G_{\mathbf{q}}^2 L^{-4}}{1 + z_0 G_{\mathbf{q}} L^{-2}} = \frac{h_0^2}{4K_c z_0^2} - k_0. \quad (18)$$

For the conjugate field of the absolute value $|m|$, we obtain the same expression with an additional term associated to the error function

$$-\frac{1}{2\bar{z}_0} + \frac{1}{2} \sum_{\mathbf{q} \neq 0} \frac{\bar{z}_0 G_{\mathbf{q}}^2 L^{-4}}{1 + \bar{z}_0 G_{\mathbf{q}} L^{-2}} = \frac{\bar{h}_0^2}{4K_c \bar{z}_0^2} - k_0 + \frac{\bar{h}_0}{2\sqrt{\pi K_c \bar{z}_0^3}} \frac{e^{-\bar{h}_0^2/(4K_c \bar{z}_0^2)}}{1 + \operatorname{erf}\left(\frac{\bar{h}_0}{2\sqrt{K_c \bar{z}_0}}\right)}. \quad (19)$$

When $h_0 = 0$, or $\bar{h}_0 = 0$, and k_0 large, the previous equations give the asymptotic solutions $z_0 \sim \bar{z}_0 \sim 1/(2k_0)$. Numerically we solved Equation (18) and Equation (19) recursively to obtain the real solution z_0 and \bar{z}_0 .

4. Cumulant expansion and asymptotic distribution

In this section we derive the cumulants from Equation (13) and given function Φ , using the constraint $\partial\Phi/\partial z = 0$ of the saddle point imposed for any conjugate field h or \bar{h} . Indeed the identity

$$\frac{d^p(\partial_z \Phi(z(h), h, 0))}{dh^p} = 0 \quad (20)$$

is valid for any integer $p \geq 0$, which simply means that at the saddle point value $z = z(h)$, $\partial_z \Phi$ is always zero as function of h . In particular, we can show recursively in Appendix B that for $p \geq 2$

$$\kappa_p = \frac{1}{N^{p-1}} \frac{d^p \bar{\Phi}}{dh^p} = \frac{1}{N^{p-1}} \sum_{k=0}^p C_p^k \frac{\partial^p \Phi}{\partial z^k \partial h^{p-k}} z'(h)^k. \quad (21)$$

Knowing the function Φ , it is straightforward to obtain the cumulant expression by derivation and summation. It is worth noting that cumulants depend only on $z(h)$ and its first derivative. From the scaling form of the distribution function, the scaling law for the cumulants (or equivalently for the moments) is $\kappa_p \sim L^{-p(d-2)/2}$. For example, $\kappa_1 = \langle m \rangle = h/(2Kz) = \frac{h_0}{2K_c z_0} L^{-(d-2)/2} = \tilde{\kappa}_1 L^{-(d-2)/2}$. We can generally use the fact that $dz(h)/dh = dz_0(h_0)/dh_0 \times L^{(d-2)/2} =: z'_0(h_0) \times L^{(d-2)/2}$, to calculate the regular part $\tilde{\kappa}_p$ of the cumulants near the critical point, and obtain for example, using Equation (B.5),

$$\frac{(-1)^p}{p!} \tilde{\kappa}_p = \frac{z_0'^p}{2pz_0^p} + \frac{z_0'^{p-2}}{4K_c z_0^{p-1}} + \frac{z_0'}{2p} \sum_{\mathbf{q} \neq 0} \frac{1}{(z_0 + L^2 G_{\mathbf{q}}^{-1})^p} - \frac{h_0 z_0'^{p-1}}{2K_c z_0^p} + \frac{h_0^2 z_0'^p}{4K_c z_0^{p+1}}, \quad (22)$$

from which we deduce the second cumulant

$$\tilde{\kappa}_2 = \frac{z_0'^2}{2z_0^2} + \frac{1}{2K_c z_0} + \frac{z_0'}{2} \sum_{\mathbf{q} \neq 0} \frac{1}{(z_0 + L^2 G_{\mathbf{q}}^{-1})^2} - \frac{h_0 z_0'}{K_c z_0^2} + \frac{h_0^2 z_0'^2}{4K_c z_0^3} \quad (23)$$

for order parameter m , and

$$\tilde{\kappa}_2 = \frac{\bar{z}_0'^2}{2\bar{z}_0^2} + \frac{1}{2K_c \bar{z}_0} + \frac{\bar{z}_0'}{2} \sum_{\mathbf{q} \neq 0} \frac{1}{(\bar{z}_0 + L^2 G_{\mathbf{q}}^{-1})^2} - \frac{1}{\pi K_c \bar{z}_0} - \frac{\bar{z}_0'}{\sqrt{\pi K_c \bar{z}_0^3}} \quad (24)$$

for order parameter $|m|$, when $\bar{h}_0 = 0$ for simplification. In the former case when $h_0 = 0$, we can show that $z_0'(0) = 0$. Indeed, deriving the saddle-point solution Equation (18), we obtain

$$z_0' \left(\frac{h_0^2}{K_c z_0^3} + \frac{1}{z_0^2} + \sum_{\mathbf{q} \neq 0} \frac{G_{\mathbf{q}}^2 L^{-4}}{(1 + z_0 G_{\mathbf{q}} L^{-2})^2} \right) = \frac{h_0}{K_c z_0^2} \quad (25)$$

for conjugate field h_0 and

$$\bar{z}_0' \left(\frac{1}{\bar{z}_0^2} + \sum_{\mathbf{q} \neq 0} \frac{G_{\mathbf{q}}^2 L^{-4}}{(1 + \bar{z}_0 G_{\mathbf{q}} L^{-2})^2} \right) = \frac{1}{\sqrt{\pi K_c \bar{z}_0^3}}. \quad (26)$$

by deriving Equation (19) and taking $\bar{h}_0 = 0$ afterward. The former equation gives $z_0'(0) = 0$, then only $\tilde{\kappa}_2 = 1/(2K_c z_0)$ is non-zero in this limit which implies that distribution $Q(\theta)$ is purely Gaussian with a variance depending on an implicit equation for z_0 . However in the latter case Equation (26), $\bar{z}_0'(0) \neq 0$ instead and $Q(\theta)$ is non-Gaussian since all the moments do not vanish. We can in general derive formally $Q(\theta)$ from definition Equation (A.3), using the expression Equation (21) for $\tilde{\kappa}_p$, and the characteristic function. We also redefine the free energy $\Phi_0 := L^d \Phi(z_0 L^{-2}, h_0 L^{-(d+2)/2})$, with

$$\Phi_0(z_0, h_0) = -\frac{1}{2} \log z_0 + \frac{1}{2} \sum_{\mathbf{q} \neq 0} \left[\frac{z_0 G_{\mathbf{q}}}{L^2} - \log \left(1 + \frac{z_0 G_{\mathbf{q}}}{L^2} \right) \right] + \frac{h_0^2}{4K_c z_0} + k_0 z_0 + \text{cst.} \quad (27)$$

For the distribution of $|m|$ and conjugate field \bar{h}_0 , we find instead

$$\begin{aligned} \bar{\Phi}_0(\bar{z}_0, \bar{h}_0) = & -\frac{1}{2} \log \bar{z}_0 + \frac{1}{2} \sum_{\mathbf{q} \neq 0} \left[\frac{\bar{z}_0 G_{\mathbf{q}}}{L^2} - \log \left(1 + \frac{\bar{z}_0 G_{\mathbf{q}}}{L^2} \right) \right] + \frac{\bar{h}_0^2}{4K_c \bar{z}_0} + k_0 \bar{z}_0 \\ & + \log \left[1 + \operatorname{erf} \left(\frac{\bar{h}_0}{2\sqrt{K_c \bar{z}_0}} \right) \right] + \text{cst.} \end{aligned} \quad (28)$$

The characteristic function H appearing in the definition of $Q(\theta)$ in Equation (A.1) has the scaling form \tilde{H} depending on Φ_0 (or $\bar{\Phi}_0$) and its derivatives

$$\tilde{H}(-\lambda) = \sum_{p \geq 2} \frac{(-i\lambda)^p}{\tilde{\kappa}_2^{p/2} p!} \tilde{\kappa}_p = \sum_{p \geq 2} \frac{(-i\lambda)^p}{\tilde{\kappa}_2^{p/2} p!} \sum_{k=0}^p C_p^k \frac{\partial^p \Phi_0}{\partial z_0^k \partial h_0^{p-k}} z_0' (h_0)^k. \quad (29)$$

The series over p can be performed directly if we use for example the Fourier transform of Φ_0

$$\begin{aligned} \Phi_0(z_0, h_0) &= \int \int \frac{dq d\omega}{(2\pi)^2} \tilde{\Phi}_0(q, \omega) \exp(iqz_0 + i\omega h_0), \\ \tilde{\Phi}_0(q, \omega) &= \int \int dz_0 dh_0 \Phi_0(z_0, h_0) \exp(-iqz_0 - i\omega h_0). \end{aligned} \quad (30)$$

Indeed, we obtain formally the functional expression of the characteristic function depending on Φ_0 only

$$\begin{aligned} \sum_{p \geq 2} \frac{(-i\lambda)^p}{\tilde{\kappa}_2^{p/2} p!} \tilde{\kappa}_p &= \int \int \frac{dq d\omega}{(2\pi)^2} \tilde{\Phi}_0(q, \omega) \exp(iqz_0 + i\omega h_0) \sum_{p \geq 2} \frac{(-i\lambda)^p}{\tilde{\kappa}_2^{p/2} p!} \sum_{k=0}^p C_p^k (iq)^k (i\omega)^{p-k} z_0' (h_0)^k \\ &= \int \int \frac{dq d\omega}{(2\pi)^2} \tilde{\Phi}_0(q, \omega) \exp(iqz_0 + i\omega h_0) \sum_{p \geq 2} \frac{(-i\lambda)^p}{\tilde{\kappa}_2^{p/2} p!} (iqz_0' + i\omega)^p \\ &= \Phi_0\left(z_0 - i \frac{\lambda z_0'}{\sqrt{\tilde{\kappa}_2}}, h_0 - i \frac{\lambda}{\sqrt{\tilde{\kappa}_2}}\right) - \Phi_0(z_0, h_0) + i \frac{\lambda}{\sqrt{\tilde{\kappa}_2}} \left(z_0' \frac{\partial}{\partial z_0} + \frac{\partial}{\partial h_0} \right) \Phi_0(z_0, h_0). \end{aligned} \quad (31)$$

This relation satisfies the constraint $\tilde{H}(0) = 0$ coming from the normalization of the PDF. It is also straightforward from Equation (A.3) to obtain the general form of the limiting distribution for conjugate fields h_0 and \bar{h}_0 as well by replacing Φ_0 by $\bar{\Phi}_0$

$$\begin{aligned} Q(\theta) &= \int \frac{d\lambda}{2\pi} \exp \left[i\lambda \left\{ \theta + \frac{1}{\sqrt{\tilde{\kappa}_2}} \frac{\partial}{\partial h_0} \Phi_0(z_0, h_0) \right\} \right. \\ &\quad \left. + \Phi_0\left(z_0 - i \frac{\lambda z_0'}{\sqrt{\tilde{\kappa}_2}}, h_0 - i \frac{\lambda}{\sqrt{\tilde{\kappa}_2}}\right) - \Phi_0(z_0, h_0) \right]. \end{aligned} \quad (32)$$

This result is convenient since the Fourier transform depends functionally only on Φ_0 which can be written for different lattice geometries or coupling distributions between the nearest-neighbor spins, by only modifying the structure of the Green function $G_{\mathbf{q}}$

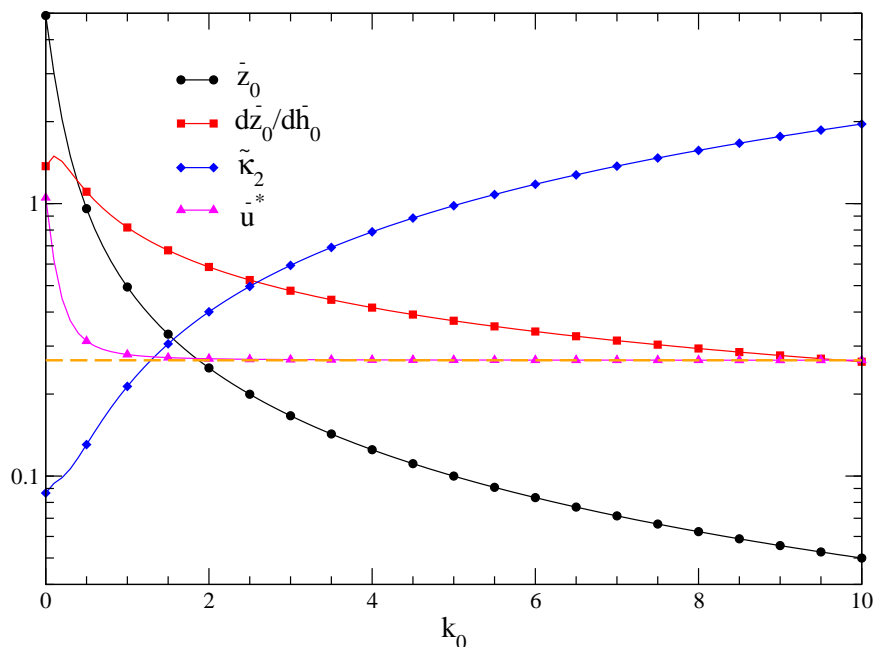


Figure 2. (Color online) plot of \bar{z}_0 , \bar{z}'_0 , $\tilde{\kappa}_2$, and asymptotic slope $\bar{u}^* = \sqrt{\tilde{\kappa}_2} \bar{z}_0 / \bar{z}'_0$ as function of k_0 for the distribution of $|m|$. In the limit of large k_0 , \bar{u}^* approaches the constant $\bar{u}^*_\infty = \sqrt{\pi(1 - 3/\pi)}/2 \simeq 0.266$ (dashed orange line, see text).

for example. Also only z_0 and z'_0 (or \bar{z}_0 and \bar{z}'_0) are necessary for the evaluation of this expression by solving Equation (18) and Equation (25) (or Equation (19) and Equation (26)). The distribution is centered around the value

$$c_0 := \frac{1}{\sqrt{\tilde{\kappa}_2}} \frac{\partial}{\partial h_0} \Phi_0(z_0, h_0) \quad (33)$$

which is equal to $c_0 = h_0 / (2\sqrt{\tilde{\kappa}_2} K_c z_0)$ using Equation (27) or $c_0 = 1 / \sqrt{\pi \tilde{\kappa}_2 K_c \bar{z}_0}$ using Equation (28) when $\bar{h}_0 = 0$ for simplification. Typical behavior of quantities \bar{z}_0 , \bar{z}'_0 , and $\tilde{\kappa}_2$ are plotted in Figure 2 after solving Equation (19) recursively.

5. Asymptotic limits and numerical results

The asymptotic analysis of Equation (32) when $\theta \gg 1$ or $\theta \ll -1$ is useful to determinate the behavior of the PDF for large deviations and obtain its universal characteristics. The standard method is to derive the argument in the exponential of the integral Equation (32) with respect with λ and look for the dominant saddle point in the complex plane. This is equivalent to analyze the existence of solutions of the following equation:

$$\begin{aligned} \theta + \frac{1}{\sqrt{\tilde{\kappa}_2}} \frac{\partial}{\partial h_0} \Phi_0(z_0, h_0) &= \frac{z'_0}{\sqrt{\tilde{\kappa}_2}} \frac{\partial \Phi_0}{\partial z_0} \left(z_0 - i \frac{\lambda z'_0}{\sqrt{\tilde{\kappa}_2}}, h_0 - i \frac{\lambda}{\sqrt{\tilde{\kappa}_2}} \right) \\ &+ \frac{1}{\sqrt{\tilde{\kappa}_2}} \frac{\partial \Phi_0}{\partial h_0} \left(z_0 - i \frac{\lambda z'_0}{\sqrt{\tilde{\kappa}_2}}, h_0 - i \frac{\lambda}{\sqrt{\tilde{\kappa}_2}} \right). \end{aligned} \quad (34)$$

The detailed analysis of this equation is given in Appendix C. We find two kinds of behavior. For $\theta \ll -1$ the PDF is exponentially decreasing $Q(\theta) \simeq \exp(u^*\theta)$ with coefficient u^* (and \bar{u}^*) equal to $u^* := \sqrt{\tilde{\kappa}_2}z_0/z'_0 > 0$ ($\bar{u}^* := \sqrt{\tilde{\kappa}_2}\bar{z}_0/\bar{z}'_0 > 0$). The saddle point structure can be checked numerically by fitting the asymptotic function given below by Equation (35) where corrections have to be taken into account for moderate $\theta < 0$ in addition to the dominant exponential term. In particular three dominant contributions are present corresponding respectively to the linear behavior discussed above, plus a term in $\sqrt{|\theta + c_0|}$, and a logarithm $\log|\theta + c_0|$:

$$Q(\theta) \simeq \exp\left(u^*\theta + \frac{\sqrt{u^*}|h_0 - u^*/\sqrt{\tilde{\kappa}_2}|}{2\sqrt{K_c z_0}}\sqrt{|\theta + c_0|} - \frac{1}{2}\log|\theta + c_0|\right), \quad \theta \ll -1. \quad (35)$$

In the opposite limit, when $\theta \gg 1$, the PDF falls off exponentially with a stretched exponent equal to $d/(d-2) = 3$ in three dimensions. The saddle point evaluation in this case is detailed in Appendix C:

$$Q(\theta) \simeq \exp\left(-\beta(d)\left(\frac{\sqrt{\tilde{\kappa}_2}}{z'_0}\theta\right)^{d/(d-2)}\right), \quad \theta \gg 1, \quad (36)$$

with eventual corrections. Here the expression of coefficient $\beta(d)$ is given by Equation (C.11), and is simply equal to $\beta(3) = 8\pi^2$ in three dimensions. These results can be checked numerically after plotting the Fourier integral Equation (32).

In Figure 3 is represented the distribution for m and for two different sets of parameters (h_0, k_0) . $Q(\theta)$ is typically non-Gaussian, with a exponential behavior for negative deviations, as expected, and more pronounced falloff for positive deviations for which a stretched exponential with a cubic exponent was performed adequately. The exponential behavior is typical to extreme value statistics when one studies the extrema distribution of a set of independent random variables, such as the Gumbel distribution. This distribution has a more pronounced asymptotic double-exponential falloff with a coefficient which is integer. Here the coefficient of θ^3 is non-integer and depends on the saddle point structure. When field h_0 is increased, negative deviations are enhanced, whereas the curve falls off more rapidly for $\theta > 0$ as the coefficient $(\sqrt{\tilde{\kappa}_2}/z'_0)^3$ in Equation (36) increases.

The distribution for $|m|$ follows the same trend. For large and negative deviations, the saddle point solution is given by Equation (C.6), with an asymptotic behavior also corresponding to Equation (35) and Equation (36). Figure 4 represents typical examples for $k_0 = 0.1$ and $k_0 = 1$ at zero field $\bar{h}_0 = 0$. The PDF is clearly non-Gaussian, and, for deviations left to the most probable value, two distinct behaviors separated by a crossover interval. When θ is largely negative, the slope of the exponential asymptote is given by \bar{u}^* , whereas there exists a plateau-like regime where the distribution, at least for $k_0 > 1/2$, takes significant values in a whole range of θ values. However, when k_0 decreases, the asymptotic regime is reached only for negative deviations that become

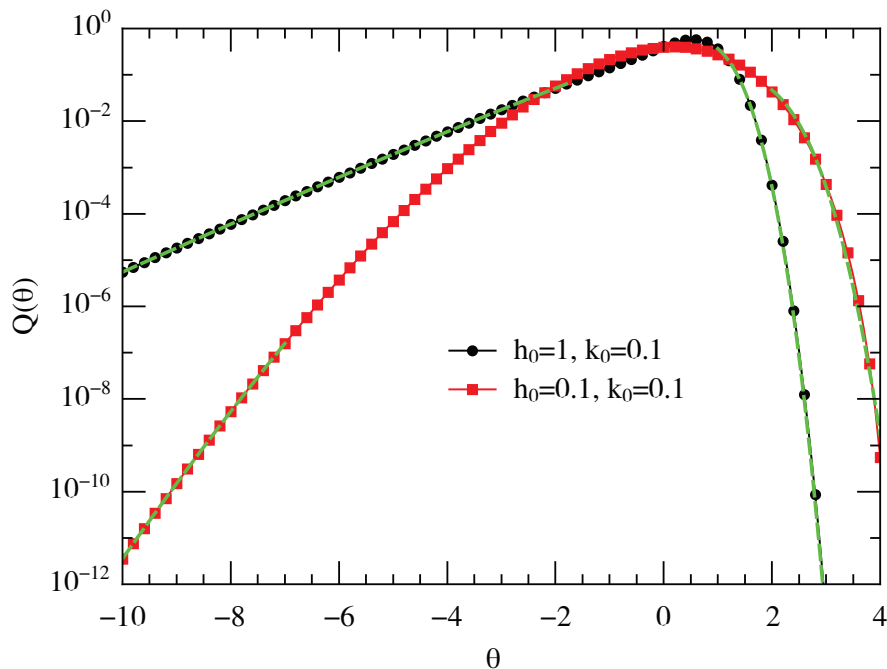


Figure 3. (Color online) plot of distribution $Q(\theta)$ Equation (32) for m and for two different sets of parameters (h_0, k_0) ($L = 10$). Dashed lines correspond to approximation curves given by asymptotic regime detailed in Appendix C. For negative deviations, the behavior is found to be exponential Equation (35) with $u^* \simeq 7.396$ for $(h_0 = 0.1, k_0 = 0.1)$ and $u^* \simeq 1.44$ for $(h_0 = 1, k_0 = 0.1)$, close to expected values $u^* = 8.15$ and $u^* = 1.45$ respectively. For positive deviations $\theta > 1$, curves are fitted with a stretched exponential with cubic exponent Equation (36).

larger and larger, as it is shown in the set of curves Figure 5 where we have varied k_0 almost continuously.

In particular, in this figure, the limit $k_0 \gg 1$ is seen to be reached for k_0 values close to 2, and the limiting distribution takes a universal form.

Indeed the saddle point values when $\bar{h}_0 = 0$ can be computed exactly in this limit since $\bar{z}_0 \sim 1/(2k_0)$, $\bar{z}'_0 \sim \sqrt{\bar{z}_0}$, and $\bar{\kappa}_2 \sim 1/\bar{z}_0$, and \bar{u}^* approaches the numerical constant $\bar{u}^*_\infty = \sqrt{\pi(1 - 3/\pi)/2} \simeq 0.266$, see Appendix C, Equation (C.7). We find that the limiting value Q_∞ of the distribution is given by

$$Q_\infty(\theta) = \int \frac{\bar{u}^* d\lambda}{2\pi} \exp \left\{ i\lambda \left(\bar{u}^* \theta + \frac{1}{\sqrt{\pi}} \right) - \frac{1}{2} \log(1 - i\lambda) - \frac{\pi\lambda^2}{4(1 - i\lambda)} + \log \left[1 - \operatorname{erf} \left(\frac{i\sqrt{\pi}\lambda}{2\sqrt{1 - i\lambda}} \right) \right] \right\}. \quad (37)$$

This integral, independent of k_0 , is a universal function of θ with numerical factors only. It is plotted in Figure 6 and presents a dominant contribution in the interval $-2.1 < \theta < 0.9$, with a sharp decreasing behavior outside this interval. The plot suggests that there may exist a cut-off at $\theta = \theta_c \simeq 0.86$ above which the distribution vanishes. We have approximated quite accurately this function by the

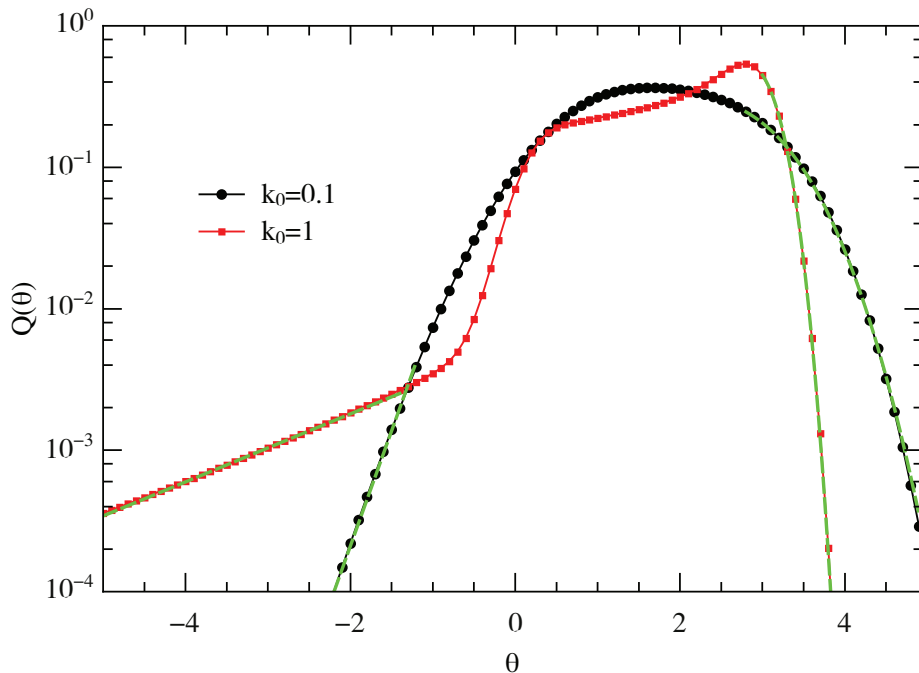


Figure 4. (Color online) plot of distribution $Q(\theta)$ Equation (32) for $|m|$ and for two different parameters k_0 ($\bar{h}_0 = 0$ and $L = 10$). Dashed lines correspond to approximation curves given by the asymptotic regime. For negative deviations, the fits are given by the exponential behavior Equation (35) with $\bar{u}^* \simeq 0.26$ for $k_0 = 1$, close to the expected value $\bar{u}^* = 0.279$. For $k_0 = 0.1$, the asymptotic regime is not reached since we expect a slope $\bar{u}^* = 0.62$, lower than the slope found in the interval $[-3, -1]$. For positive deviations $\theta > 1$, curves are fitted accurately with a stretched exponential with cubic exponent Equation (36).

Ansatz $Q_\infty(\theta) \approx \exp\{a\theta - b/(\theta - \theta_c)\}/(\theta_c - \theta)^\alpha$ in the interval $\theta > -2$, with fitted parameters $a = 0.055$, $b = 0.0351$, $\theta_c = 0.8533$ and $\alpha = 0.826$.

Finally, in Figure 7, we have plotted the distribution of m for a series of several h_0 values at $k_0 = 0$. As discussed above, the distribution for $(h_0 = 0, k_0 = 0)$ is a Gaussian, and differs from the Gaussian form as the field is increased, and presents asymptotically the exponential form Equation (35) for large negative deviations. However the structure is different from Figure 5 since no plateau regions are present.

6. Conclusion

In this paper, we presented an analytical method to compute the distribution function of the magnetization in the spherical model at criticality, with a numerical application in three dimensions. The advantage of this spin-correlated model is that the critical region can be explored analytically leading to important properties of the PDF. In particular, the exponential behavior for large and negative deviations are characteristic of the presence of soft modes $|\mathbf{q}| \ll 1$ destroying the long-range order as seen in the 2D-XY model, with additional corrections not seen usually in extreme statistics distributions of uncorrelated variables. For larger deviations, the PDF is falling off more rapidly than

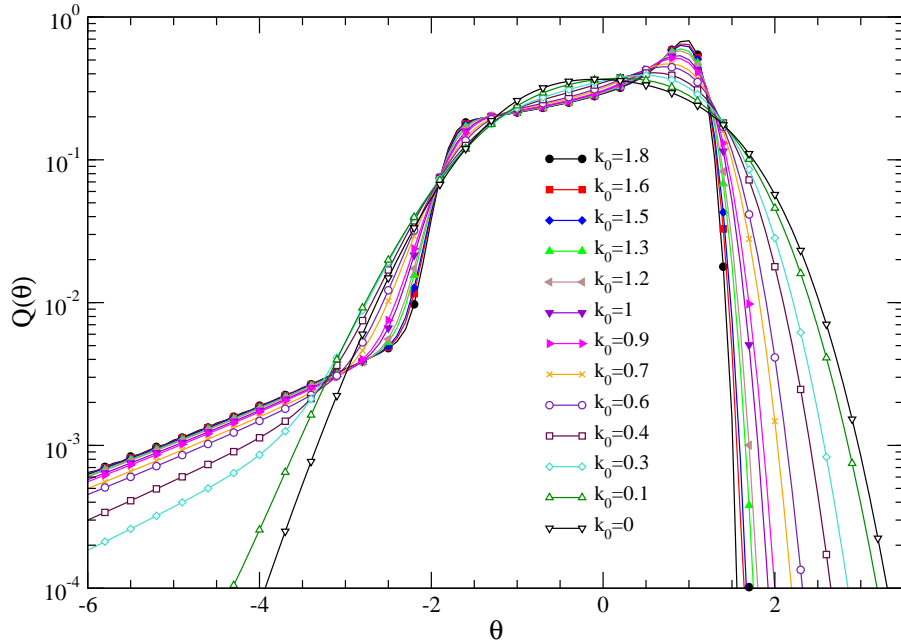


Figure 5. (Color online) multiple plots of the distribution $Q(\theta)$ for $|m|$ and for several values of k_0 ($\bar{h}_0 = 0$ and $L = 10$). A crossover occurs around $k_0 = 0.5$ below which the plateau-like feature of the distribution is smoothed out. The large k_0 limit is almost reached when k_0 is larger than 2 (see also Figure 6).

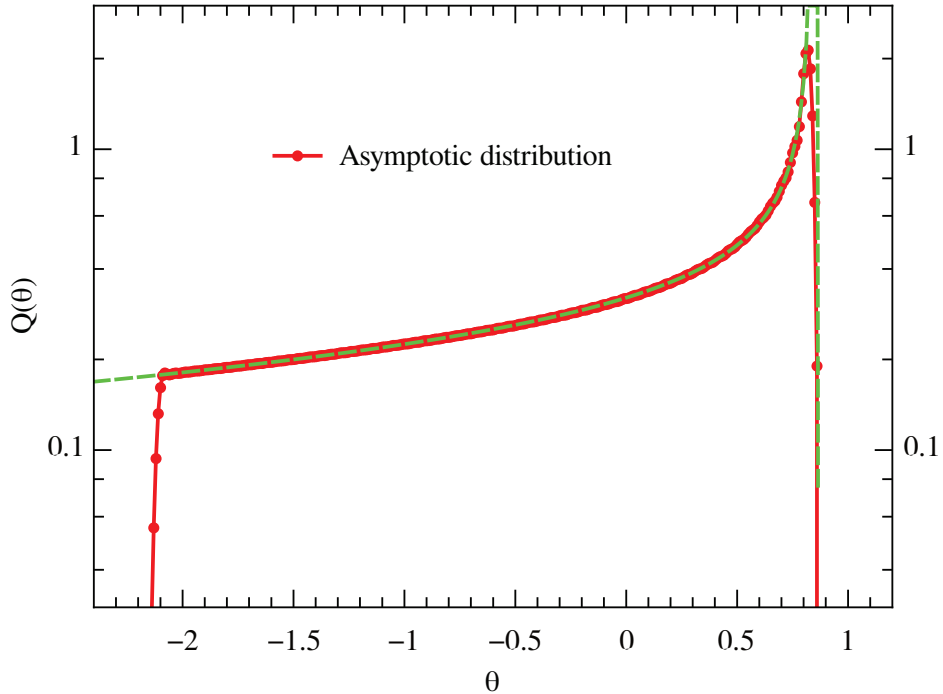


Figure 6. (Color online) plot of the distribution $Q_\infty(\theta)$ Equation (37) in the limit of large k_0 ($\bar{h}_0 = 0$ and $L = 10$). Dashed blue line corresponds to the approximate function $Q_\infty(\theta) \approx \exp\{a\theta - b/(\theta - \theta_c)\}/(\theta_c - \theta)^\alpha$ in the interval $\theta < \theta_c$, with parameters $a = 0.055$, $b = 0.0351$, $\theta_c = 0.8533$, and $\alpha = 0.826$.

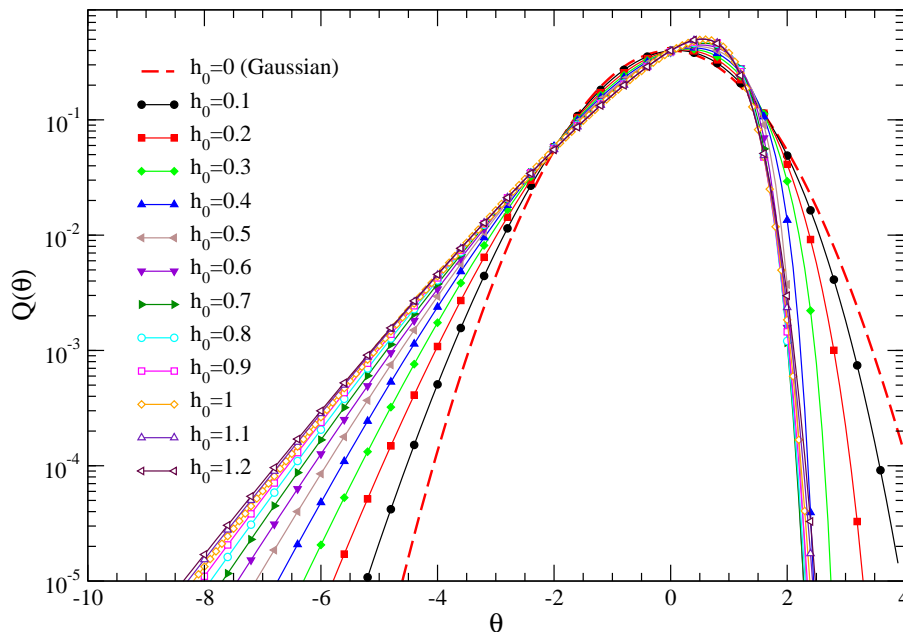


Figure 7. (Color online) multiple plots of the m distribution $Q(\theta)$ for several values of h_0 ($k_0 = 0$ and $L = 10$). The distribution at $h_0 = 0$ is purely Gaussian $Q(\theta) = \exp(-\theta^2/2)/\sqrt{2\pi}$ (see text).

a Gaussian, as the long-range order is more difficult to restore. The stretched exponent of the exponential falloff depends on the dimension like $d/(d-2)$. When $d = 4$ the Gaussian behavior is recovered, and when d is close to two dimensions, the exponent is diverging, and we expect formally a double exponential falloff in this limit for positive deviations, as for the 2D-XY model and 2D Ising model as well [23]. By inspection of the partition function in the Fourier space Equation (5), we can reformulate the problem and associate the PDF as the distribution of a set of uncorrelated Fourier modes $S_{\mathbf{q}}$ which appear in the integrand. However these modes are coupled by the variable of integration s coming from the constraint over the spins, which leads, a priori, to a PDF which is not a standard distribution. It seems nonetheless that using a saddle point analysis in the large size limit we obtain the PDF of quasi-independent modes not evenly distributed, which implies strongly non-Gaussian characteristics in the general case [19]. We found for the spherical model that the PDF belongs to a class of functions closely related to Gumbel but with a stretched exponential for positive deviations instead of a double exponential form when the dimension is larger than two. Moreover the corrective terms found asymptotically for negative deviations in Equation (35) may originate from the correlations between modes and induced by the constraint over the spins.

The main result Equation (32), giving formally the Fourier expression of the PDF, can be applied for any model where a saddle point analysis is exact, since the cumulants can be expressed simply with a generating function, see Appendix B. This model can moreover be modified in order to incorporate additional couplings or crystal fields for example. In this case, only the rescaled free energies given by Equation (27) and

Equation (28) have to be reformulated to accommodate the modifications made in the original Hamiltonian.

Appendix A. Limiting distribution

Cumulant κ_p are defined by the characteristic function H of instantaneous spin order parameter $\sum_i S_i/N$

$$\mathbb{E} \left[e^{i\lambda \sum_i S_i/N} \right] = \exp[H(\lambda)] = \exp \left(\sum_{p \geq 1} \kappa_p \frac{(i\lambda)^p}{p!} \right) \quad (\text{A.1})$$

where $\mathbb{E}[\cdot]$ is the thermal average operator over the different spin configurations and κ_p the cumulants. The distribution $P(m, L)$ can then be expressed as the Fourier transform of $\exp[H(-\lambda)]$

$$\begin{aligned} P(m, L) &:= \int \frac{d\lambda}{2\pi} \exp[i\lambda m + H(-\lambda)] \\ &= \int \frac{d\lambda}{2\pi} \exp \left[i\lambda m + \sum_{p \geq 1} \kappa_p \frac{(-i\lambda)^p}{p!} \right]. \end{aligned} \quad (\text{A.2})$$

If $\kappa_p = 0$ for all $p > 2$, $P(m, L)$ is Gaussian and κ_2 is the variance σ^2 , $P(m, L) = \exp \left[-\frac{(m-\kappa_1)^2}{2\kappa_2} \right] / \sqrt{2\pi\kappa_2}$ or $P(m, L) = Q \left(\theta := \frac{(m-\kappa_1)}{\sqrt{\kappa_2}} \right) / \sqrt{\kappa_2}$, where $Q(\theta) = \exp(-\theta^2/2) / \sqrt{2\pi}$ is the normalized Gaussian distribution function. In general, we expect the distribution to be non-Gaussian if $\kappa_{p \geq 3} \neq 0$, and $P(m, L)$ can be put generally into the following form using the rescaled cumulants defined in Equation (13)

$$\begin{aligned} P(m, L) &= L^{\beta/\nu} \int \frac{d\lambda}{2\pi\sqrt{\tilde{\kappa}_2}} \exp \left[i\lambda \frac{(m-\kappa_1)}{\sqrt{\kappa_2}} + \sum_{p \geq 2} \frac{\tilde{\kappa}_p}{\tilde{\kappa}_2^{p/2}} \frac{(-i\lambda)^p}{p!} \right] \\ &= L^{\beta/\nu} \int \frac{d\lambda}{2\pi\sqrt{\tilde{\kappa}_2}} \exp \left[i\lambda\theta + \sum_{p \geq 2} \frac{\tilde{\kappa}_p}{\tilde{\kappa}_2^{p/2}} \frac{(-i\lambda)^p}{p!} \right] =: L^{\beta/\nu} \frac{1}{\sqrt{\tilde{\kappa}_2}} Q(\theta), \end{aligned} \quad (\text{A.3})$$

with $\beta/\nu = (d-2)/2$ for the spherical model.

Appendix B. Cumulant expression

In this appendix, we derive the exact differential relation Equation (21). Consider the p^{th} cumulant of the distribution as the derivative of the $(p-1)^{\text{th}}$ one, using the assumption that Equation (21) is correct for κ_{p-1}

$$\begin{aligned}
N^{p-1}\kappa_p &= \frac{d}{dh} \left(\sum_{k=0}^{p-1} C_{p-1}^k \frac{\partial^{p-1}\Phi}{\partial z^k \partial h^{p-1-k}} z'(h)^k \right) \\
&= \sum_{k=0}^{p-1} C_{p-1}^k \left[\frac{\partial^p \Phi}{\partial z^{k+1} \partial h^{p-1-k}} z'(h)^{k+1} + \frac{\partial^p \Phi}{\partial z^k \partial h^{p-k}} z'(h)^k + \frac{\partial^{p-1}\Phi}{\partial z^k \partial h^{p-1-k}} k z'(h)^{k-1} z''(h) \right].
\end{aligned} \tag{B.1}$$

The first two terms in the last line can be brought together using the binomial formula $C_{p-1}^{k-1} + C_{p-1}^k = C_p^k$ and rearranging the summation index k . We then obtain

$$N^{p-1}\kappa_p = \sum_{k=0}^p C_p^k \frac{\partial^p \Phi}{\partial z^k \partial h^{p-k}} z'(h)^k + z''(h) \sum_{k=0}^{p-1} k C_{p-1}^k \frac{\partial^{p-1}\Phi}{\partial z^k \partial h^{p-1-k}} z'(h)^{k-1}. \tag{B.2}$$

Using $k C_{p-1}^k = (p-1) C_{p-2}^{k-1}$, we can show that the last term is equal to

$$\begin{aligned}
z''(h) \sum_{k=1}^{p-1} k C_{p-1}^k \frac{\partial^{p-1}\Phi}{\partial z^k \partial h^{p-1-k}} z'(h)^{k-1} &= z''(h) \sum_{k=1}^{p-1} (p-1) C_{p-2}^{k-1} \frac{\partial^{p-1}\Phi}{\partial z^k \partial h^{p-1-k}} z'(h)^{k-1} \\
&= z''(h) (p-1) \frac{d^{p-2} \partial_z \Phi}{dh^{p-2}}.
\end{aligned} \tag{B.3}$$

This term is equal to zero at the saddle point value, proving the recurrence for Equation (21) at order p . Now, if we consider the first expression for Φ in Equation (7), the dependence in h is quadratic, and only 3 terms remain from Equation (21)

$$\kappa_p = \frac{1}{N^{p-1}} \left[\frac{\partial^p \Phi}{\partial z^p} z'^p + p \frac{\partial^p \Phi}{\partial z^{p-1} \partial h} z'^{p-1} + \frac{1}{2} p(p-1) \frac{\partial^p \Phi}{\partial z^{p-2} \partial h^2} z'^{p-2} \right]. \tag{B.4}$$

Using for example the exact expression for $\Phi(z, h, 0)$, we can compute the cumulants as function of the saddle point z and its derivative $z'(h)$ only

$$\begin{aligned}
\frac{(-1)^p}{p!} \kappa_p &= \frac{z'^p}{2p N^p z^p} + \frac{z'^{p-2}}{4K N^{p-1} z^{p-1}} + \frac{z'^p}{2p} \frac{1}{N^p} \sum_{\mathbf{q} \neq 0} \frac{1}{(z + d - \sum_{\alpha} \cos q_{\alpha})^p} \\
&\quad - \frac{h z'^{p-1}}{2K N^{p-1} z^p} + \frac{h^2 z'^p}{4K N^{p-1} z^{p+1}}.
\end{aligned} \tag{B.5}$$

This result can be used in Equation (A.2) to obtain the characteristic function $H(-\lambda)$ by re-summation over p of the cumulant series.

Appendix C. Asymptotic analysis

The asymptotic solutions for the saddle point equation Equation (34) can be derived when $\theta \ll -1$ and $\theta \gg 1$. In both cases, the left hand side of Equation (34) proportional to θ is diverging negatively and positively respectively, which leads us to look for a

diverging solution for the right hand side as well. For the two cases considered in this paper, Equation (34) is equal to

$$\theta + \frac{1}{\sqrt{\tilde{\kappa}_2}} \frac{h_0}{2K_c z_0} = \frac{z'_0}{\sqrt{\tilde{\kappa}_2}} \left[-\frac{1}{2Z_0} + \frac{1}{2} \sum_{\mathbf{q} \neq 0} \frac{G_{\mathbf{q}}^2}{L^4} \frac{Z_0}{1 + Z_0 G_{\mathbf{q}}/L^2} - \frac{H_0^2}{4K_c Z_0^2} + k_0 \right] + \frac{1}{\sqrt{\tilde{\kappa}_2}} \frac{H_0}{2K_c Z_0}, \quad (\text{C.1})$$

and

$$\theta + \frac{1}{\sqrt{\tilde{\kappa}_2 \pi K_c \bar{z}_0}} = \frac{\bar{z}'_0}{\sqrt{\tilde{\kappa}_2}} \left[-\frac{1}{2\bar{Z}_0} + \frac{1}{2} \sum_{\mathbf{q} \neq 0} \frac{G_{\mathbf{q}}^2}{L^4} \frac{\bar{Z}_0}{1 + \bar{Z}_0 G_{\mathbf{q}}/L^2} - \frac{\bar{H}_0^2}{4K_c \bar{Z}_0^2} + k_0 \right] - \frac{\bar{H}_0}{2\sqrt{\pi K_c \bar{Z}_0^{3/2}} \frac{e^{-\bar{H}_0^2/(4K_c \bar{Z}_0)}}{1 + \operatorname{erf}\left(\frac{\bar{H}_0}{2\sqrt{K_c \bar{Z}_0}}\right)}} + \frac{1}{\sqrt{\tilde{\kappa}_2}} \left[\frac{\bar{H}_0}{2K_c \bar{Z}_0} + \frac{1}{\sqrt{\pi K_c \bar{Z}_0}} \frac{e^{-\bar{H}_0^2/(4K_c \bar{Z}_0)}}{1 + \operatorname{erf}\left(\frac{\bar{H}_0}{2\sqrt{K_c \bar{Z}_0}}\right)} \right], \quad (\text{C.2})$$

where

$$Z_0 = z_0 - i \frac{\lambda z'_0}{\sqrt{\tilde{\kappa}_2}}, \quad \bar{Z}_0 = \bar{z}_0 - i \frac{\lambda \bar{z}'_0}{\sqrt{\tilde{\kappa}_2}} \\ H_0 = h_0 - i \frac{\lambda}{\sqrt{\tilde{\kappa}_2}}, \quad \bar{H}_0 = -i \frac{\lambda}{\sqrt{\tilde{\kappa}_2}}. \quad (\text{C.3})$$

Considering first the regime $\theta \ll -1$, let assume in the following that z_0 and z'_0 are positive (as well as \bar{z}_0 and \bar{z}'_0), which will be realized numerically by solving Equation (18) and Equation (25). We are looking at diverging terms in the previous saddle point equation coming from the inverse powers of $Z_0 \simeq 0$ or $\bar{Z}_0 \simeq 0$ for example. Considering the integration path C^- in the complex plane for λ (see Figure C1), it is clear there is a special point on the negative imaginary axis $\lambda = -iu^*$ with $u^* := \sqrt{\tilde{\kappa}_2} z_0/z'_0 > 0$ ($\bar{u}^* := \sqrt{\tilde{\kappa}_2} \bar{z}_0/\bar{z}'_0 > 0$) for which $Z_0 = 0$ and the right hand side of Equation (C.1) (and Equation (C.2)) is singular.

The most singular term appears to be the one proportional to $1/Z_0^2 \propto 1/(u^* - u)^2$, after setting $\lambda = -iu$ with u close enough to u^* , and which gives the estimate for the saddle point solution

$$u \simeq u^* - \frac{\sqrt{u^*} |h_0 - u^*/\sqrt{\tilde{\kappa}_2}|}{2\sqrt{K_c z_0} |\theta + c_0|}. \quad (\text{C.4})$$

Replacing this value in Equation (32) and integrating the Gaussian fluctuations around the saddle point, we obtain the dominant contribution for the large negative deviations Equation (35).

The asymptotic behavior of the PDF is therefore exponentially decreasing, with a coefficient equal to u^* . The same analysis for Equation (C.2) leads to a similar result,

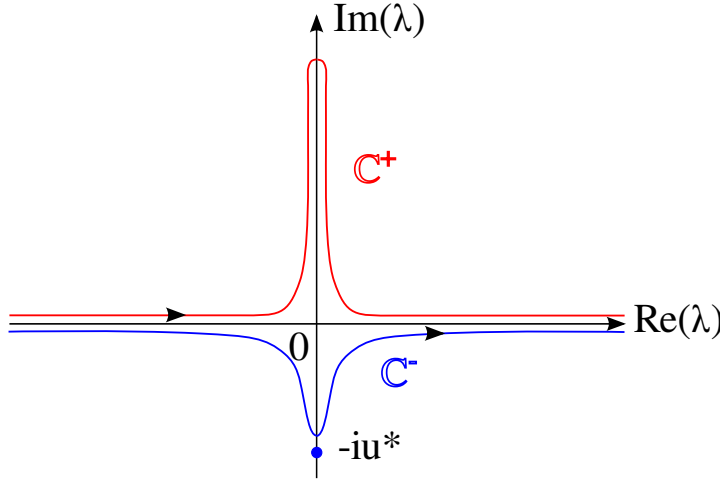


Figure C1. (Color online) modified path of integration for the saddle point analysis. C^+ is the path chosen when $\theta \gg 1$ and C^- when $\theta \ll -1$.

with coefficient \bar{u}^* instead. The inverse powers in Equation (C.1) and Equation (C.2) appear to be indeed only in $1/Z_0$, $1/Z_0^{1/2}$, $1/Z_0^{3/2}$, and $1/Z_0^2$, with the latter one being the dominant contribution. The additional two terms in Equation (C.2) proportional to

$$\frac{e^{-\bar{H}_0^2/(4K_c\bar{Z}_0)}}{1 + \operatorname{erf}\left(\frac{\bar{H}_0}{2\sqrt{K_c\bar{Z}_0}}\right)} \simeq \frac{e^{-\bar{u}^{*3}/[4K_c\tilde{\kappa}_2\bar{z}_0(\bar{u}^*-u)]}}{1 - \operatorname{erf}\left(\bar{u}^{*3/2}/[2\sqrt{K_c\tilde{\kappa}_2\bar{z}_0}(\bar{u}^*-u)]\right)} \quad (\text{C.5})$$

are singular in the limit $u \rightarrow \bar{u}^*$ since both numerator and denominator vanish. However this ratio can be evaluated using the asymptotic behavior of the error function for large and negative argument. This ratio diverges like $1/\bar{Z}_0^{1/2}$ and elevates the power of the factor $1/\bar{Z}_0^{3/2}$ in the second line in Equation (C.2), giving rise to a dominant contribution proportional to $1/\bar{Z}_0^2$, in addition to the identical contribution proportional to \bar{H}_0^2/\bar{Z}_0^2 found in the first line. Finally, the saddle point solution is given by

$$u \simeq \bar{u}^* - \frac{\bar{u}^*\sqrt{\bar{u}^*}}{\sqrt{2K_c\bar{z}_0}|\theta + c_0|}. \quad (\text{C.6})$$

instead of Equation (C.4) and for $\bar{h}_0 = 0$ only. Since Z_0 is small, the sum term over modes \mathbf{q} in the saddle point equations is regular since it behaves in this limit like $Z_0\tilde{g}_2$ with \tilde{g}_2 finite. It is no more the case in $d \geq 4$ where \tilde{g}_2 is diverging logarithmically with the system size and where a careful different analysis has to be made for the new saddle point, and where one expects to find a Gaussian behavior with a θ^2 contribution.

Considering the PDF of $|m|$ in absence of field $\bar{h}_0 = 0$, we can estimate the asymptotic value of \bar{u}^* when k_0 is large. Indeed, from Equation (19) we obtain the approximation $\bar{z}_0 \simeq 1/(2k_0) \ll 1$, and from Equation (26), $\bar{z}'_0 \simeq \sqrt{\bar{z}_0/(\pi K_c)}$. In addition, the second cumulant is equal to $\tilde{\kappa}_2 \simeq (1 - 3/\pi)/(2K_c\bar{z}_0)$. Then we obtain the universal limit

$$\lim_{k_0 \rightarrow \infty} \bar{u}^* =: \bar{u}_\infty^* = \sqrt{\frac{\pi}{2} \left(1 - \frac{3}{\pi}\right)} \simeq 0.266. \quad (\text{C.7})$$

In the regime of large and positive deviations $\theta \gg 1$, the previous analysis can not be valid anymore because of the sign of θ . Instead we are looking for a path C^+ in the upper complex plane $\Im(\lambda) > 0$ where Z_0 is real and large. Indeed since θ is large, we can assume that the modulus of $\lambda =: iu$ becomes large as well, so that $Z_0 \simeq uz'_0/\sqrt{\tilde{\kappa}_2} \gg 1$. In this case, terms proportional to inverse powers of Z_0 in Equation (C.1) and Equation (C.2) are small or finite, except the sum over the \mathbf{q} modes. This sum contributes like $\sum_{\mathbf{q} \neq 0} G_{\mathbf{q}}/L^2$ which diverges with the system size when $d \geq 2$. Indeed $g_1 = \sum_{\mathbf{q} \neq 0} G_{\mathbf{q}}/L^d$ is finite for $d > 2$ and diverges logarithmically when $d = 2$. Therefore the former sum is divergent with Z_0 . Since $Z_0 > 0$ when $\lambda = iu$ with $u > 0$, the sign of the function

$$F(Z_0) = \sum_{\mathbf{q} \neq 0} \frac{G_{\mathbf{q}}^2}{L^4} \frac{Z_0}{1 + Z_0 G_{\mathbf{q}}/L^2} \quad (\text{C.8})$$

is positive and consistent with the sign of θ on the left hand side of Equation (C.1), and the saddle point equations reduces to $\theta \simeq z'_0 F(Z_0)/(2\sqrt{\tilde{\kappa}_2})$. The divergent part of $F(Z_0)$ can be evaluated exactly in the continuous limit. Indeed, we can rewrite Equation (C.8) as an integral

$$F(Z_0) \simeq \frac{L^d S_d}{(2\pi)^d} \int_{\text{cst}/L}^{\text{cst}} dq q^{d-1} \frac{4}{q^4 L^4} \frac{Z_0}{1 + 2Z_0/(q^2 L^2)}, \quad (\text{C.9})$$

where $S_d = 2\pi^{d/2}/\Gamma(d/2)$ is the hyper-spherical volume. Performing the change of variable $qL/\sqrt{2Z_0} \rightarrow q$ and taking afterward the limit $L \rightarrow \infty$, we obtain typically

$$F(Z_0) \simeq \frac{S_d 2^{d/2}}{(2\pi)^d} \int_{\text{cst}/\sqrt{2Z_0}}^{\infty} dq \frac{q^{d-3}}{1+q^2} Z_0^{(d-2)/2} \simeq \frac{\pi Z_0^{(d-2)/2}}{(2\pi)^{d/2} \Gamma(d/2) \cos[\pi(d+1)/2]}, \quad (\text{C.10})$$

where the integral can be computed in general dimension $2 < d < 4$ after substituting the lower bound with zero. Then the saddle point is given by

$$\begin{aligned} u &\simeq \left\{ (2/\pi)(2\pi)^{d/2} \Gamma(d/2) \cos[\pi(d+1)/2] \right\}^{2/(d-2)} \left(\frac{\sqrt{\tilde{\kappa}_2}}{z'_0} \right)^{d/(d-2)} \theta^{2/(d-2)} \gg 1 \\ &=: \beta(d) \left(\frac{\sqrt{\tilde{\kappa}_2}}{z'_0} \right)^{d/(d-2)} \theta^{2/(d-2)}. \end{aligned} \quad (\text{C.11})$$

After inserting this value in Equation (32), we finally obtain the dominant behavior of the PDF given by the stretched exponential Equation (36).

References

- [1] Archambault P, Bramwell S T, Fortin J Y, Holdsworth P C W, Peysson S and Pinton J F 1998 *Journal of Applied Physics* **83** 7234–7236 URL <http://link.aip.org/link/?JAP/83/7234/1>
- [2] Bramwell S T, Christensen K, Fortin J Y, Holdsworth P C W, Jensen H J, Lise S, López J M, Nicodemi M, Pinton J F and Sellitto M 2000 *Phys. Rev. Lett.* **84**(17) 3744–3747 URL <http://link.aps.org/doi/10.1103/PhysRevLett.84.3744>
- [3] Bramwell S T, Fortin J Y, Holdsworth P C W, Peysson S, Pinton J F, Portelli B and Sellitto M 2001 *Phys. Rev. E* **63**(4) 041106 URL <http://link.aps.org/doi/10.1103/PhysRevE.63.041106>
- [4] Berezinskii V L 1971 *Sov. Phys. JETP* **32** 493
- [5] Thouless D J and Kosterlitz J M 1973 *J. Phys. C: Solid State Phys.* **6** 1181
- [6] José J V, Kadanoff L P, Kirkpatrick S and Nelson D R 1977 *Phys. Rev. B* **16**(3) 1217–1241 URL <http://link.aps.org/doi/10.1103/PhysRevB.16.1217>
- [7] Bramwell S T, Holdsworth P C W and Pinton J F 1998 *Nature (London)* **396** 552
- [8] Antal T, Droz M, Györgyi G and Rácz Z 2001 *Phys. Rev. Lett.* **87**(24) 240601 URL <http://link.aps.org/doi/10.1103/PhysRevLett.87.240601>
- [9] Bertin E 2005 *Phys. Rev. Lett.* **95** 170601
- [10] Bertin E and Clusel M 2006 *J. Phys. A* **39** 7607–7619
- [11] Bak P, Tang C and Wiesenfeld K 1987 *Phys. Rev. Lett.* **59**(4) 381–384 URL <http://link.aps.org/doi/10.1103/PhysRevLett.59.381>
- [12] Jensen H J 1998 *Self-Organized Criticality* (Cambridge University Press)
- [13] Seneta E 1969 *Adv. Appl. Probab.* **1** 1
- [14] Biggins J D and Bingham N H 1993 *Adv. Appl. Proba.* **25** 757–772
- [15] Barabási A L and Albert R 1999 *Science* **286** 509–512
- [16] Rácz Z and Plischke M 1994 *Phys. Rev. E* **50**(5) 3530–3537 URL <http://link.aps.org/doi/10.1103/PhysRevE.50.3530>
- [17] Kim J S, Goh K I, Salvi G, Oh E, Kahng B and Kim D 2007 *Phys. Rev. E* **75** 016110
- [18] Jo J, Fortin J Y and Choi M Y 2011 *Phys. Rev. E* **83**(3) 031123 URL <http://link.aps.org/doi/10.1103/PhysRevE.83.031123>
- [19] Clusel M and Bertin E 2008 *Int. Journ. of Mod. Phys. B* **22** 3311–3368
- [20] Plischke M, Rácz Z and Zia R K P 1994 *Phys. Rev. E* **50**(5) 3589–3593 URL <http://link.aps.org/doi/10.1103/PhysRevE.50.3589>
- [21] Berlin T H and Kac M 1952 *Phys. Rev.* **86**(6) 821–835 URL <http://link.aps.org/doi/10.1103/PhysRev.86.821>
- [22] Baxter B J 1989 *Exactly Solved Models in Statistical Mechanics* (Academic Press) ISBN 0120831821
- [23] Clusel M, Fortin J Y and Holdsworth P C W 2006 *EPL (Europhysics Letters)* **76** 1008 URL <http://stacks.iop.org/0295-5075/76/i=6/a=1008>